JOURNAL OF GEOPHYSICAL RESEARCH, VOL. 88, NO. C5, PAGES 2827–2835, MARCH 30, 1983

Turbulent Heat and Momentum Transfer in the Oceanic Boundary Layer Under Melting Pack Ice

MILES G. MCPHEE

Naval Postgraduate School, Monterey, California 93940

A theory for momentum flux in the planetary boundary layer (PBL) stabilized by continuous surface buoyancy is extended to include turbulent flux of an arbitrary scalar contaminant and then used to estimate how wind-driven sea ice melts as it encounters temperatures in the oceanic boundary layer that are above the melting point. Given wind stress and temperature difference $\Delta\theta$ across the oceanic PBL, the theory predicts melt rate and ice drift velocity. Results indicate that the effect of buoyancy on PBL turbulence is significant even with small values of $\Delta\theta$ (<0.5 K). Curves of melt rate and ice speed as functions of u_*, the interfacial friction velocity, show that melting is strongly dependent on stress at the interface and that the effective drag on the ice undersurface is significantly reduced at oceanic temperatures commonly observed in the marginal ice zone. The latter suggests that divergence will occur at the ice margin when off-ice winds advect the pack over water above the melting temperature. The structure of mean currents beneath the ice is also investigated; results indicate that advection will play an important, if not dominant, role in determining water column properties near an ice edge front.

1. INTRODUCTION

Large horizontal gradients in near-surface ocean temperature are often a prominent feature of the marginal ice zone (MIZ). *Paquette and Bourke* [1979], during a summer cruise in the Chukchi Sea, found the sea surface temperature to change by over 6 K across a distance of about 25 km as the ice concentration fell from seven-eighths cover to zero. This is an enormous gradient by most oceanic standards, and under such conditions it is clear that heat transfer from ice to ocean is an important factor in determining where the ice margin occurs and how it will evolve. Nor is the existence of significant temperature gradients confined to summer: *Pease* [1980] found changes of about 1 K over 10 km across the ice margin in the Bering Sea during March 1979 and also reported that the ice rotted rapidly when it encountered the warmer water, even when other thermodynamic factors that would cause decay were small.

The melting of sea ice in contact with water above the melting temperature occurs by heat transfer across a turbulent planetary boundary layer (PBL) at scales for which the Coriolis effect cannot be ignored, and the problem has several additional features that make it interesting from the viewpoint of boundary layer physics. A complex interplay exists between the melting induced by heat transfer from the relatively warm water and the simultaneous influx of fresh meltwater. By acting to stabilize PBL turbulence the 'negative salinity flux' associated with the meltwater tends to retard heat transfer. The same effect lessens the efficiency with which turbulent stress is transferred, with the result that the effective drag on the ice is reduced. If the strength of the stabilizing influence depends on the temperature difference across the boundary layer (as it should), then because advancing ice cools the water behind it, the leading edge should encounter less drag than the ice following, creating a potential divergence at the ice margin due solely to turbulence dynamics in the oceanic boundary layer.

The intent of the present work is to determine whether the tendencies described above reach significant quantitative levels under conditions that might realistically be found at the ice margin. The results suggest that oceanic boundary layer dynamics can indeed have a notable impact on the thermodynamic regime in the MIZ.

The theory developed here is based on recent work [*McPhee*, 1981] in which a simplified mixing length model was used to develop an analytic similarity theory for momentum transfer in the PBL subjected to stabilizing buoyancy flux at the surface, conditions characteristic both of the nocturnal atmospheric boundary layer when there is surface radiational cooling and of pack ice drifting across water warm enough to cause melt. The present task is to extend the analytic theory to include, in a fairly general way, a description for the flux of a scalar contaminant in the boundary layer and then to apply those principles to the specific problem of ice melt and temperature change in the boundary layer.

From the original theory [*McPhee*, 1981] the following nondimensional variables provide a unique solution for stress and velocity (except in a thin, near-surface layer) in a steady, horizontally homogeneous boundary layer under varying conditions of surface (interfacial) kinematic stress $\hat{\tau}_0 = u_*\hat{u}_*$ (carets denote complex numbers) and surface buoyancy flux represented by Obukhov length L. (See the notation list for other definitions.)

Stress

$$\hat{T} = \hat{\tau}/u_*\hat{u}_*$$

Depth

$$\zeta = fz/u_*\eta_* \tag{1}$$

Velocity

$$\hat{u} = \eta_*\hat{U}/\hat{u}_*$$

Eddy viscosity

$$K_* = fK_m/u_*^2\eta_*^2$$

Similarity is achieved by specifying the nondimensional eddy viscosity as a 'universal' constant: $K_* = k\xi_N$, where ξ_N

Paper number 2C1340.
0148-0227/83/002C-1340$05.00

is the nondimensional surface layer extent, about one eighth of the total boundary layer thickness. In the surface layer the physical length scale z_0 plays a role, so that for fluid near the interface, velocity does vary in the nondimensional representation. (In other words, near-surface profiles are not similar.) The parameter η_* is a stability parameter which indicates the reduction of the maximum mixing length from its neutrally stable value ($\xi_N u_*/f$), given by

$$\eta_* = (1 + \xi_N u_*/R_c f L)^{-1/2}$$

Note that surface buoyancy enters the PBL solution through the Obukhov length

$$L = \rho_0 u_*^3/(gk\langle\rho' w'\rangle|_0) \tag{2}$$

where $\langle\rho' w'\rangle|_0$ is the turbulent flux of density variation at the interface. Nondimensional profiles for mean stress and velocity in the oceanic PBL are

$$\hat{T} = e^{\hat{\delta}\zeta}$$

$$\hat{u} = -i\hat{\delta}e^{\hat{\delta}\zeta} \qquad \zeta \le -\xi_N$$

$$\hat{u} = -i\hat{\delta}e^{-\hat{\delta}\xi_N} - \frac{\eta_*}{k}$$

$$\cdot\left[\ln\frac{|\zeta|}{\xi_N} + (\hat{\delta} - a)(\zeta + \xi_N) + \frac{a}{2}\hat{\delta}(\zeta^2 - \xi_N^2)\right] \qquad \zeta > -\xi_N$$

The nondimensional surface velocity, which is in effect the turbulent drag law for the sea ice, is given by

$$\hat{u}_0 = \frac{\eta_* \hat{U}_0}{\hat{u}_*} = -i\hat{\delta}e^{-\hat{\delta}\xi_N} - \frac{\eta_*}{k}$$

$$\cdot\left[\ln\frac{|\zeta_0|}{\xi_N} + (\hat{\delta} - a)\xi_N + \frac{a}{2}\hat{\delta}\xi_N^2\right] \tag{3}$$

where $\hat{u}_0$ represents the change in nondimensional velocity across the PBL.

2. Extension of the Similarity Theory to Scalar Contaminants

The relationship between the mean gradient of a scalar property of the boundary layer (e.g., temperature, salinity, or some other contaminant) and the turbulent flux of that property is treated like the momentum flux, by invoking Reynold's analogy, wherein the eddy exchange coefficient appropriate to turbulent transfer of the contaminant is assumed to be proportional to the eddy viscosity. Let λ be an arbitrary quantity of which there is a surface flux denoted by $\langle w'\lambda'\rangle|_0$. The turbulent flux is related to the mean gradient by

$$\langle w'\lambda'\rangle = -K_\lambda \frac{\partial\lambda}{\partial z} = -klu_\lambda \frac{\partial\lambda}{\partial z} \tag{4}$$

where u_λ is an effective turbulent mixing velocity for the property λ ($u_\lambda = u_*$ when the property is vector momentum), so that $u_\lambda = \gamma_\lambda u_*$, where

$$\gamma_\lambda = K_\lambda/K_m$$

K_m being the eddy viscosity. The expression for turbulent flux is thus

$$\langle w'\lambda'\rangle = -\gamma_\lambda K_m \,\partial\lambda/\partial z$$

To fit turbulent diffusion of λ into the similarity theory, it is nondimensionalized as follows: Let H be the nondimensional flux of λ at any level, defined by $H = \langle w'\lambda'\rangle/\langle w'\lambda'\rangle|_0$, and let λ_* be the scale for λ, so that the nondimensional value is $\Lambda = \lambda/\lambda_*$. Equation (4) is nondimensionalized using the scales of section 1:

$$H = \frac{\langle w'\lambda'\rangle}{\langle w'\lambda'\rangle|_0} = -\left(\frac{\gamma_\lambda u_* \eta_* \lambda_*}{\langle w'\lambda'\rangle|_0}\right) K_* \frac{\partial\Lambda}{\partial\zeta}$$

It is convenient to choose λ_* so that the expression in parentheses is unity, that is,

$$\lambda_* = \langle w'\lambda'\rangle|_0/\gamma_\lambda u_* \eta_*$$

and the flux/mean gradient relationship is

$$H = -K_* \,\partial\Lambda/\partial\zeta$$

Note that the factor γ_λ (which for the case where λ represents temperature is the inverse of the turbulent Prandtl number) is contained in the scaling and does not appear in the dimensionless equation.

The question then arises of how the nondimensional flux varies through the PBL. In what follows, two hypotheses are developed, each of which can be argued plausibly. In section 3 it is shown that the results of both approaches are similar, so the distinction is mainly heuristic.

Hypothesis 1 (Used in 'Standard Case')

For the first hypothesis we simply extend the analogy with momentum flux and assume that the nondimensional contaminant flux profile is similar to that of scalar momentum flux. This has an advantage in that only one new 'external' parameter, namely, γ_λ, enters the problem.

From the similarity theory the solution for turbulent momentum flux is

$$\hat{T} = e^{\hat{\delta}\zeta} = e^{(2k\xi_N)^{-1/2}\zeta} \cdot e^{i(2k\xi_N)^{1/2}\zeta}$$

and the scalar equation is $T = e^{b\zeta}$, where $b = (2k\xi_N)^{-1/2}$. By analogy, $H = e^{b\zeta}$. Note that the difference in turbulent diffusion rates is accounted for by γ_λ in λ_*.

The mean profile is obtained in the same way that the velocity profile was. For the outer layer

$$\frac{\partial\Lambda}{\partial\zeta} = -(1/k\xi_N)e^{b\zeta}$$

$$\Lambda(\zeta) - \Lambda_\infty = -(2/k\xi_N)^{1/2}e^{b\zeta}$$

where Λ_∞ is the far-field value of Λ. Let the subscript *sl* refer to the value at the maximum extent of the surface layer (i.e., $\zeta = -\xi_N$), which is the top of the Ekman layer. Then

$$\Lambda_{sl} - \Lambda_\infty = -(2/k\xi_N)^{1/2}e^{-(\xi_N/2k)^{1/2}} \tag{5}$$

In the surface layer,

$$\langle w'\lambda'\rangle = \frac{\gamma_\lambda k z u_*}{1 + (\beta|z|/L)} \cdot \frac{\partial\lambda}{\partial z} \qquad \zeta > -\xi_N$$

which is nondimensionalized to

$$H = \frac{k}{\eta_*}(1 - \beta\mu_*\eta_*\zeta)^{-1}\zeta\frac{\partial\Lambda}{\partial\zeta} = e^{b\zeta} \simeq 1 + b\zeta$$

so that

$$\frac{\partial \Lambda}{\partial \zeta} = \frac{\eta_*}{k\zeta}(1 + b\zeta)(1 - a\zeta)$$

where the exponential is approximated by the first two terms of a Taylor series expansion, since $|\zeta|$ is small. This is integrated from the level $\zeta = -\xi_N$ to get

$$\Lambda(\zeta) - \Lambda_{sl} = \frac{\eta_*}{k} \cdot \left[\ln \frac{|\zeta|}{\xi_N} + (b - a)(\zeta + \xi_N) - \frac{ab}{2}(\zeta^2 - \xi_N^2)\right] \quad (6)$$

With $|\zeta_0| \ll \xi_N$ the total change in Λ across the PBL is the sum of changes across the outer and surface layers, namely,

$$\Lambda_0 - \Lambda_\infty = -(2/k\xi_N)^{1/2} e^{-(\xi_N/2k)^{1/2}} + \frac{\eta_*}{k}\left[\ln \frac{|\zeta_0|}{\xi_N} + (b - a)\xi_N + \frac{ab}{2}\xi_N^2\right] \quad (7)$$

Hypothesis 2

The second hypothesis is that the scalar flux falls off linearly from its surface value to zero at the maximum nondimensional PBL depth. The second approach acknowledges that in most observations a fairly sharp gradient in a contaminant at the base of a 'mixing layer' develops with time, especially if the contaminant has an active effect on turbulence through buoyancy. This indicates a finite depth limit to the capacity for mixing by surface-driven turbulence rather than a purely exponential decay. Using Arctic Ice Dynamics Joint Experiment (AIDJEX) data, we showed [*McPhee*, 1982] that this limit appeared to be close to a nondimensional depth of about 0.4, in agreement with atmospheric studies such as *Zilitinkevich*'s [1975] work.

Here the nondimensional flux decreases linearly from its surface value to zero at ζ_D. (This implies that with constant surface fluxes the property will be uniformly distributed in time throughout the mixing layer.)

$$H = 1 - \zeta/\zeta_D$$

where ζ_D is the maximum nondimensional PBL depth. The integral across the outer layer is thus

$$\Lambda_{sl} - \Lambda_D = \frac{1}{k}\left[\frac{\zeta_D}{2\xi_N} + \left(1 + \frac{\xi_N}{2\zeta_D}\right)\right]$$

In the surface layer the flux falloff is linear, so the change across the surface layer is like (6) except that b is replaced by $b_1 = -1/\zeta_D$. With these modifications the total change across the PBL for the second hypothesis is

$$\Lambda_0 - \Lambda_\infty = \frac{\eta_*}{k}\left[\ln \frac{|\zeta_0|}{\xi_N} + (b_1 - a)\xi_N + \frac{ab_1}{2}\xi_N^2\right] - \frac{1}{k}\left[\frac{\zeta_D}{2\xi_N} + \left(1 + \frac{\xi_N}{2\zeta_D}\right)\right] \quad (8)$$

Equations (7) and (8) are scalar analogs of the vector 'drag law' (equation (3)).

3. Application

In this section the similarity theory is applied to an idealized problem in which a compact, uniform sea ice cover drifts across an abrupt front in oceanic temperature at the ice margin. The task is to calculate the velocity and melt rate of the ice, given stress at the interface and the ambient temperature of the seaward water. The temperature structure of the water column beneath the ice is also considered.

The heat flux from water to ice can be expressed in terms of the ice growth rate d as follows. We assume that all the interfacial heat flux goes to melting sea ice; then

$$\rho_0 c_p \langle w'\theta'\rangle|_0 = \rho_i L_i d$$

where L_i is the latent heat of melting for saline ice, c_p is the specific heat of water, and $\rho_0 c_p \langle w'\theta'\rangle|_0$ is the turbulent heat flux at the ice/water interface. Let Q_θ be a 'kinematic' latent heat

$$Q_\theta = \rho_i L_i/\rho_0 c_p$$

Then the kinematic turbulent heat flux at the interface is

$$\langle w'\theta'\rangle|_0 = -Q_\theta d$$

From consideration of the turbulent conservation law for salinity, the salinity flux at the interface can similarly be expressed in terms of d:

$$\langle w'S'\rangle|_0 = -d[S_w - (\rho_i/\rho_0)S_i]/1000 = -Q_s d$$

where S_w and S_i are the salinities of the boundary layer and the ice, respectively, expressed in parts per thousand.

An approximate expression for the equation of state of seawater is

$$(\rho - \rho_0)/\rho_0 = -\alpha_\theta(\theta - \theta_0) + \alpha_s(S - S_0)$$

where ρ_0, θ_0, and S_0 are reference values for density, temperature, and salinity; therefore

$$\frac{\langle \rho' w'\rangle|_0}{\rho_0} = -\alpha_\theta \langle w'\theta'\rangle|_0 + \alpha_S \langle w'S'\rangle|_0 = (\alpha_\theta Q_\theta - \alpha_S Q_S)d \quad (9)$$

From (9) the melt rate affects the turbulent structure through the Obukhov length (equation (2)), and the dimensionless parameter $\mu_* = u_*/fL$ is given by

$$\mu_* = (gk/\rho_0 f u_*^2)(\alpha_\theta Q_\theta - \alpha_S Q_S)d$$

Parameters η_* and a are calculated directly from μ_* and u_*; with u_* and d specified, the nondimensional velocity change is given by (3), and the actual velocity (relative to undisturbed water below the PBL) and other variables are found using the scales (1). Examples for different values of μ_* are given by *McPhee* [1981].

The vertical profile of scalar temperature is treated similarly: given u_* and d, the change in nondimensional temperature across the boundary layer is given by either (7) or (8), depending on which hypothesis is chosen to represent the falloff of nondimensional heat flux. The temperature scale is given by (4):

$$\theta_* = -Q_\theta d/\gamma_\theta u_* \eta_*$$

so that the temperature change across the PBL is

$$\Delta\theta = -(Q_\theta d/\gamma_\theta u_* \eta_*)(\Lambda_S - \Lambda_\infty)$$

The nondimensional expressions (7) and (8) pertain as well

to salinity, the surface flux of which is also tied to the growth rate d, so that

$$\Delta S = (\gamma_\theta Q_S / \gamma_S Q_\theta)\Delta\theta$$

But note that the factor γ_S introduces another degree of freedom connected with turbulence. There is little reason to think that γ_S equals γ_θ; indeed, observations, especially of double diffusive structure in turbulent flows, indicate that γ_S is significantly less than γ_θ, that is that turbulent diffusion of salt is slower than turbulent diffusion of heat [e.g., *Turner*, 1973, chapter 8].

As posed, the practical problem is to find from u_* and $\Delta\theta$ (i.e., $\theta_S - \theta_\infty$) the growth rate d and from it to deduce other boundary layer characteristics including surface drift. This is accomplished by an iterative process as follows. First, assume that buoyancy has no effect on the turbulence so that $\eta_* = 1$ and $a = 0$, and calculate the nondimensional temperature change across the PBL, $\Delta\Theta = \Lambda_S - \Lambda_\infty$, from (9). The trial temperature scale is $\theta_* = \Delta\theta/\Delta\Theta$, from which the growth rate is

$$d = -\gamma_\theta \eta_* u_* \Delta\theta/(Q_\theta \Delta\Theta)$$

With this furnishing an initial estimate of the buoyancy effect, $\Delta\Theta$ and θ_* are recalculated, giving a refined estimate for d. The procedure is repeated until the change in $\Delta\Theta$ from the previous iteration is less than a specified tolerance.

The relationship among u_*, melt rate, and surface drift speed as predicted by the model developed above is investigated in a series of parameter studies designed to determine which effects caused the most pronounced response in the model. Constant values were assigned to the following quantities: $k = 0.4$, $R_c = 0.2$, $\xi_N = 0.052$, $g = 980$ cm s^{-2}, $\alpha_s = 0.8$, $\rho_i = 0.9$ g cm^{-3}, $\rho_0 = 1.03$ g cm^{-3}, $S_w = 31‰$, $S_i = 7‰$, $\theta_s = -0.5$°C, and $f = 1.3 \times 10^{-4}$ s^{-1} (corresponding to latitude 64°). The coefficient of thermal expansion, α_θ, was calculated from the average temperature in the surface layer using an approximation of Table 3.1 from *Neumann and Pierson* [1966], but for temperature ranges studied, thermal expansion had little effect on buoyancy flux. For surface layer temperatures near 0°C, α_θ can be ignored.

The remaining parameters, θ_∞, Q_θ, γ_θ, and z_0, were varied through plausible ranges. In addition, a comparison was made between the two hypotheses for the heat flux profile in the boundary layer.

Figure 1 shows ice speed and melt rate plotted versus u_*

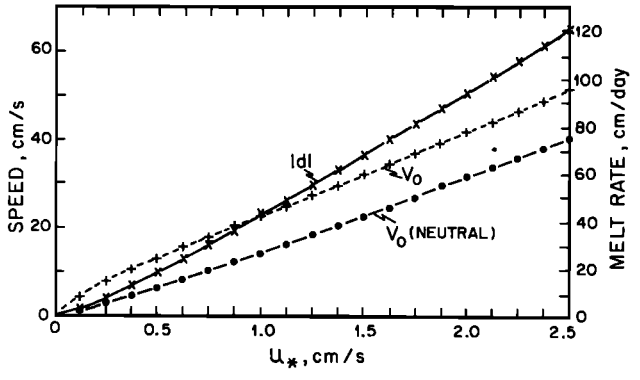

Fig. 1. Ice speed and melt rate as a function of u_* (the square root of the kinematic interfacial stress) for the 'standard' case: $\Delta\theta = 1$ K, $Q_\theta = 65$ K, $z_0 = 5$ cm, and $\gamma_\theta = 1$. The curve labeled V_0(neutral) is ice speed with no melting, $\Delta\theta = 0$.

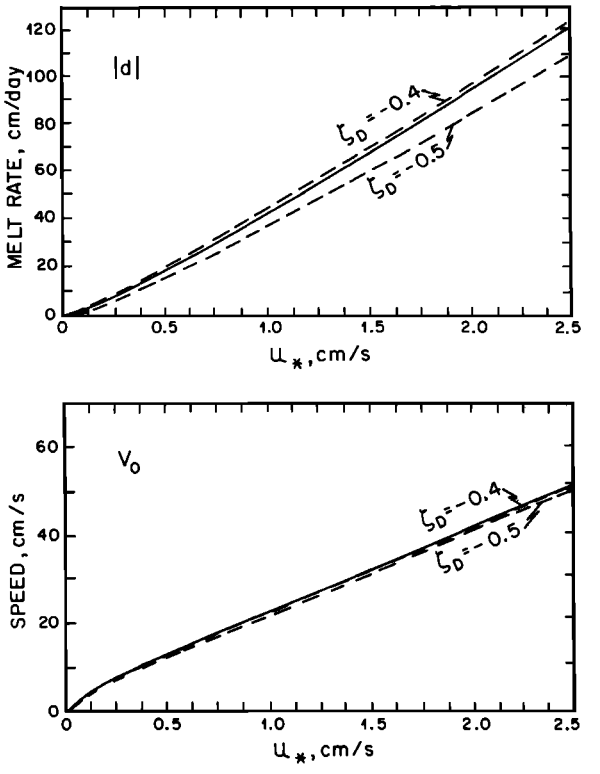

Fig. 2. Ice speed and melt rate for the standard case with exponential heat flux falloff in PBL (solid curves) and with linear flux falloff assuming nondimensional PBL depth ζ_D as indicated. Here $\zeta_D = -0.4$ corresponds to maximum PBL extent implied by AIDJEX summer data.

for the 'standard case,' that is, exponential flux falloff (use of (6)): $\theta_\infty = 0.5$°C ($\Delta\theta = 1$ K), $Q_\theta = 65$ K, $z_0 = 5$ cm, and $\gamma_\theta = 1$. Also shown is the speed that would be expected with no buoyancy effect from surface melting, that is, with a neutral PBL. As a rough guide, u_* is approximately proportional to surface wind (if the ice is not too thick), and the range shown covers winds up to about 35 kn (~65 km/h). For the standard case where the temperature change across the PBL is 1 K, the ice drifts about 60% faster than it would with no melting and ablates at a rate of 43 cm/d when the interfacial stress is 1 dyn cm^{-2}.

Figure 2 demonstrates that which hypothesis is chosen to describe the heat flux falloff in the mixing layer is not a major factor in the model. The choice of 0.4 for the nondimensional PBL thickness is consistent with atmospheric studies [e.g., *Zilitinkevich*, 1975] and with AIDJEX studies of the ice/ocean boundary layer [*McPhee*, 1982]. It coincides closely with results obtained assuming an exponential falloff.

Figure 3 shows a parameter study in which surface speed and melt rate are plotted against u_* for three different values of the far-field temperature: 0°, 0.5°, and 1.0°C. The central curve in each part represents the standard case. Both the relative speed and the melt rate increase with $\Delta\theta$, but not proportionately. This is demonstrated more clearly by Figure 4, where the melt rate is calculated as a function of $\Delta\theta$, first with u_* constant (Figure 4*a*) and then with the surface speed held constant (Figure 4*b*).

Figure 4 demonstrates how the turbulence-suppressing tendency of the meltwater affects heat transfer and also provides a departure point for relating the present results to laboratory studies of heat transport in wallbounded shear

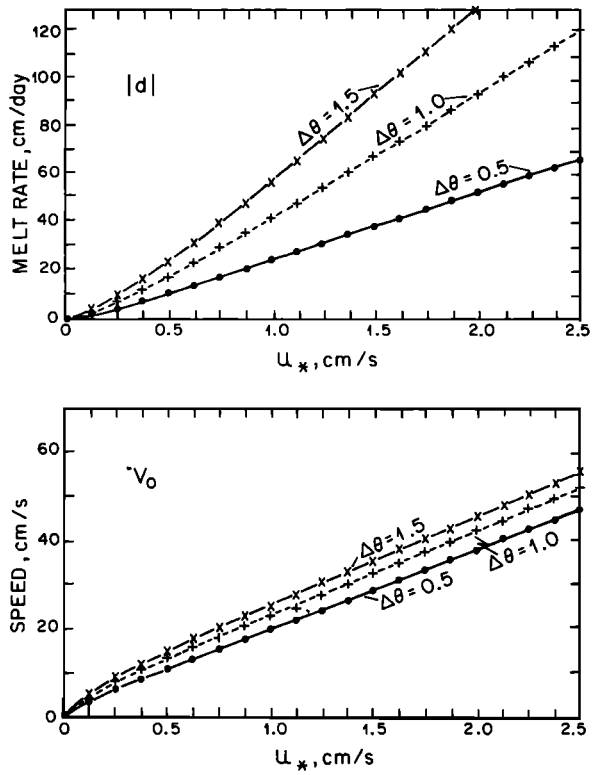

Fig. 3. Parameter study showing effect of variation in $\Delta\theta$ on ice speed and melt rate. The curves labeled $\Delta\theta = 1.0$ correspond to the standard case of Figure 1.

flows. It is customary to express heat transfer in the laboratory situation by the bulk expression [*Hinze*, 1975]

$$\langle w'\theta' \rangle = c_h V_0 \Delta\theta$$

The heat transfer coefficient c_h (Stanton number) is usually found to have a weak Reynolds number dependence [e.g., *Ashton*, 1972], where the Reynolds number is $Re = V_0 X/v$, X being a physical length scale characterizing the flow and v the molecular kinematic viscosity. If we envision an experiment where we vary the temperature of a flow with constant velocity at a set depth in a flume, then the above remarks imply that heat flux measured from a surface held at a different temperature should vary linearly with the water temperature in the flume, because Re remains constant. In terms of turbulent transfer, the mixing length remains nearly constant, and surface flux of a passive contaminant (heat) is proportional to the mean far-field concentration. *Griffin* [1978] obtained essentially this result in a theoretical investigation of iceberg ablation using a model in which density variation and rotation were ignored. His theory suggested that for the same towing speed, a berg would melt slightly more than twice as fast when the far-field temperature was 10°C rather than 5°C.

Figure 4*b* demonstrates that the present theory predicts quite different behavior. The turbulent heat transfer is markedly less efficient at higher values of $\Delta\theta$, despite the fact that surface speed remains constant. The physical explanation derives from the fact that at higher melt rates both the turbulent intensity u_*/V_0 and the mixing length relative to V_0/f are smaller. The latter effect is apparent in Figure 4*a*, where u_* rather than surface speed is constant. In the model, buoyancy flux becomes important as the Obukhov length decreases relative to the other pertinent scales of the problem, and the capacity of the turbulence to transfer heat is reduced.

The latent heat of fusion for sea ice, unlike that for fresh ice, is not constant. It depends on the brine volume and the temperature of the ice/brine mixture near the interface and may differ from the latent heat of formation [*Schwerdtfeger*, 1964]. Precise specification of the amount of heat required to melt a given thickness of ice is thus a difficult problem, avoided here by treating the 'kinematic' latent heat Q_θ as a variable parameter. For pure ice at the freezing point, Q_θ is about 71 K. Normally, the value would be smaller for saline ice, unless heat was being conducted toward the surface, in which case the effective latent heat might exceed the pure value. Figure 5, which shows surface speed and melt rate for three values of Q_θ, from 55 K to 75 K, demonstrates that uncertainty in latent heat has small effect on calculated surface speed but moderate impact for melt rate.

Another thermodynamic parameter of considerable importance to the turbulent properties of the flow is γ_θ, the inverse of the turbulent Prandtl number, which like many other properties of turbulence is not well known. *Hinze* [1975] cites studies of pipe flow turbulence with various fluids (with molecular Prandtl numbers ranging from 0.03 to 14) in which the turbulent Prandtl numbers clustered about unity. The curves in Figure 6, computed with γ_θ values from 0.5 to 2, show that melt rate in the model is quite sensitive to this parameter, which is not surprising, since it and turbulent heat flux are directly proportional. Surface speed is less strongly affected.

The final parameter study deals with the effective surface roughness z_0, which is also difficult to assess. The value reported for the AIDJEX Main Experiment stations by *McPhee* [1979] was about 10 cm, but this included integrated effects like increased drag due to pressure ridge keels.

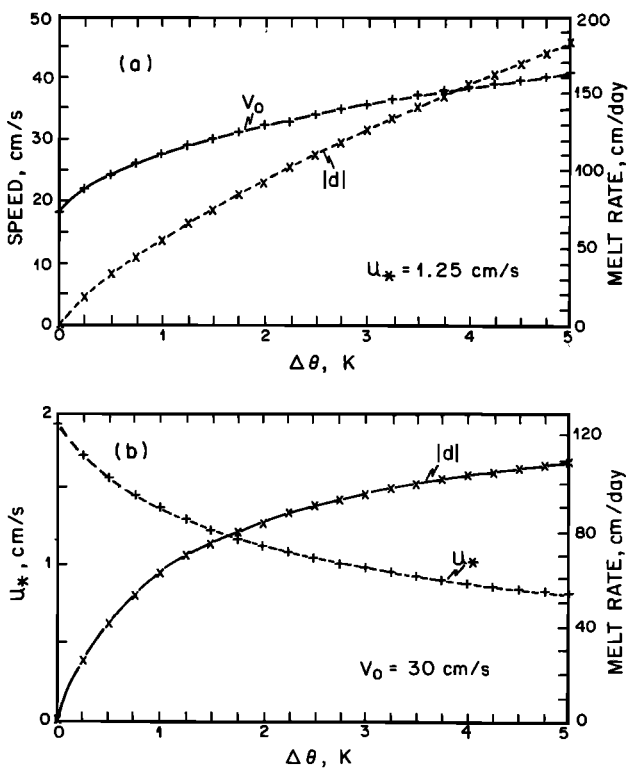

Fig. 4. (*a*) Melt rate and u_* as functions of change in temperature across the PBL for fixed surface speed $V_0 = 30$ cm s^{-1}. (*b*) Melt rate and surface speed for fixed $u_* = 1.25$ cm s^{-1}.

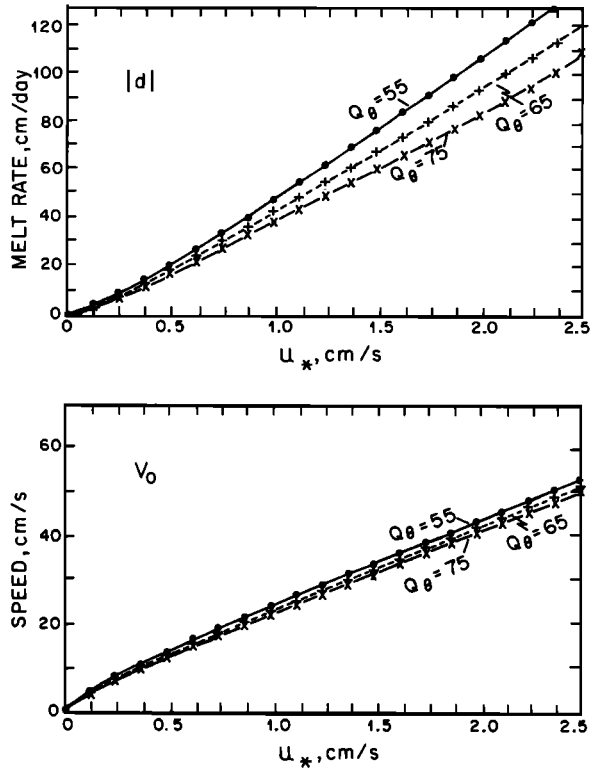

Fig. 5. Parameter study with variable Q_θ, the 'kinematic' latent heat.

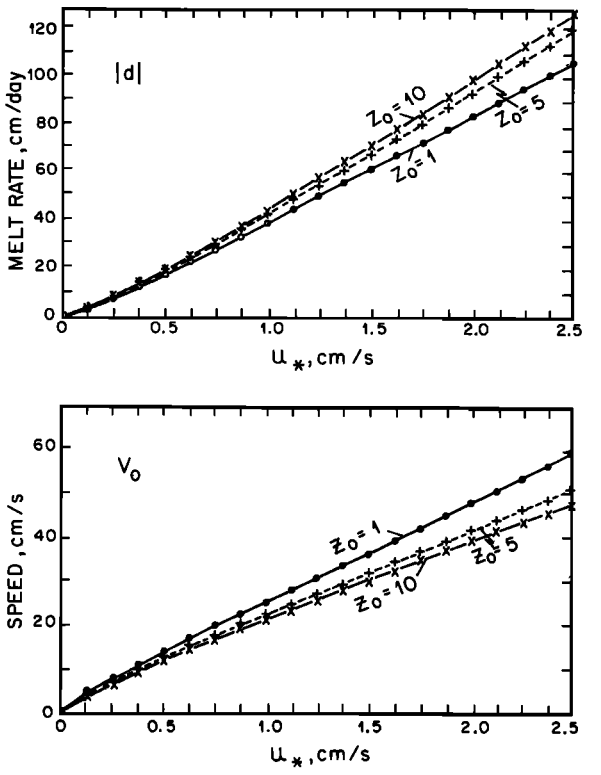

Fig. 7. Parameter study with variable z_0, the effective under-ice surface roughness.

Locally smooth floes probably have much smaller values [*McPhee and Smith*, 1976]. Another factor, addressed in more detail later, is the possibility that the melting process itself changes z_0 appreciably. Figure 7 shows that an order-of-magnitude change in z_0 causes a relatively weak response in the model. Of the parameters varied, this is the only case in which an inverse correlation between changes in speed and melt rate exists. Increasing the roughness increases the relative turbulent intensity for the same interfacial stress; thus the ice slows and melts more rapidly.

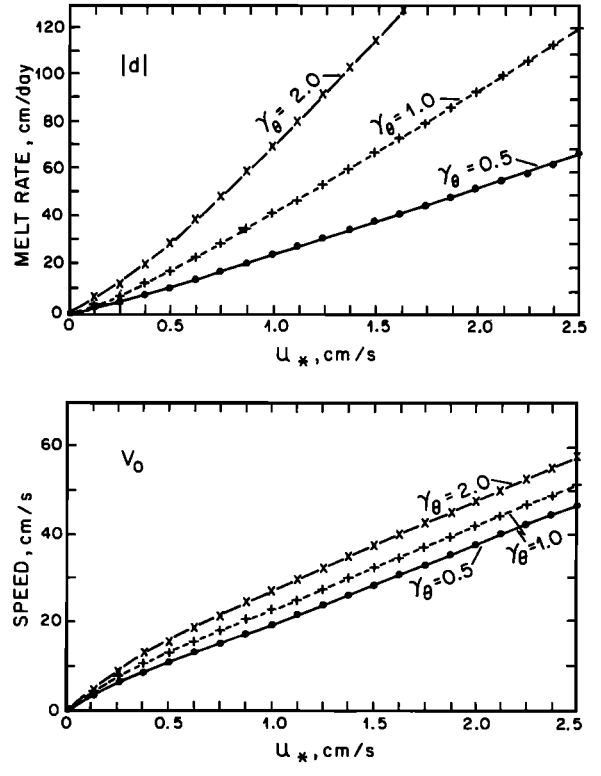

Fig. 6. Parameter study with variable γ_θ, the ratio of the turbulent heat diffusivity to the eddy viscosity.

So far we have specified the stress at the interface between the ice and water, but more often the accessible property is the wind stress acting at the ice surface; therefore it is germane to ask how the momentum of the ice modifies the drift regime, especially as the ice ablates. The problem is addressed by solving the boundary layer relations in conjunction with an ice momentum balance in which the Coriolis force on the ice column is included. No account of internal stress gradients in the ice itself is taken, as it seems unlikely that such forces would be important for ice drifting toward open water. The effect of inertial forces in the ice/boundary layer system, which is also ignored, cannot be passed off so lightly, but if time scales of the order of the inertial period are considered, then the average motion should not depart greatly from a steady-state simulation.

The steady balance of forces on an ice column of unit area is

$$if\rho_i h_i \hat{V}_0 = \hat{\tau}_a - \rho_0 u_* \hat{u}_* \tag{10}$$

where $\hat{\tau}_a$ is the air stress and h_i is the ice thickness ($d = dh_i/dt$). Equation (10) is solved, after specifying a constant wind stress, initial ice thickness, and fair-field temperature, by iterating from an initial guess for u_*. Since the ice ablates, the problem is time dependent is one sense, and the ice trajectory will curve slightly as the force balance adjusts.

Figure 8 shows 24-hour trajectories of ice drift for three cases under constant wind stress of magnitude 2 dyn cm^{-2}

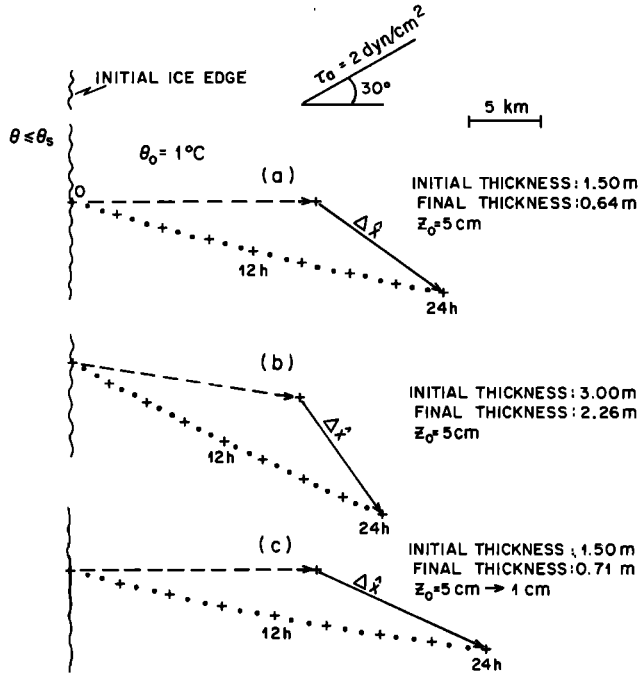

Fig. 8. Ice floe trajectory calculated for 24 hours with an off-ice wind of 2 dyn cm^{-2}, as shown, for ice drifting across an abrupt ocean temperature change at the initial ice edge. Dashed vectors show the trajectory with no melting: $\Delta\hat{x}$ indicates relative displacements of the leading edge with respect to floes in the interior pack. In Figure 8c the under-ice surface roughness decreases from 5 to 1 cm in the first 3 hours.

toward the direction shown. In the first, ice initially 1.5 m thick drifts across a front at $t = 0$ beyond which the water temperature is 1°C. The dashed line represents the straight displacement if there were no melting (neutral stability); the potential separation after 24 hours between ice at the leading edge and ice in the interior is shown by the arrow labeled $\Delta\hat{x}$. Note that the leading edge drifts away seaward, but with a clockwise deflection. Behavior like this has been described at a melting ice edge in the Bering Sea by *Martin et al.* [1981], although they attribute the downwind separation to absorption of wind wave radiation stress. The ice thins to about 64 cm over the 24 hours, which accounts for the slight leftward curvature after the initial deflection caused by the change in boundary layer scales (see *McPhee* [1981] for more details regarding the effect of buoyancy on surface deflection).

In the second case the initial thickness is 3 m, which changes the force balance enough to cause a noticeable decrease in divergence. The same bottom surface roughness was used as for the first case (5 cm), the rationale being that an expected increase in bottom roughness of thicker ice would be offset by a similar increase in the wind drag.

The final trajectory is like the first, except that during the first 3 hours of drift, the under-ice surface roughness decreases linearly from 5 cm to 1 cm. One can surmise that during rapid melting, erosion would tend to smooth the undersurface; the effect is included using the somewhat arbitrary numbers above. The result is to increase the separation and to decrease the rightward deflection.

In order to estimate how the ice trailing behind the advancing edge behaves, one needs some idea of how the water column is cooled by the rapid melting. This problem is quite complex and clearly beyond the limited scope of the analytic model as it is developed here; however, the concepts outlined above can be used to make some qualitative observations.

First, it is tempting to treat the introduction of meltwater as a simple one-dimensional mixing problem. Figure 9 shows how the average temperature and depth of the mixing layer would behave under two limiting assumptions regarding the depth to which the mixing occurs. In the first the depth of the PBL is set by the dynamic constraint, $\zeta_D = -0.4$, when the ice first encounters the warm water and remains there. The thought is that a salinity-stabilized pycnocline would develop at about that depth in a short time that would effectively limit subsequent turbulent mixing to levels above the pycnocline. In that case the change in average temperature is simply the time integral of the kinematic surface heat flux divided by the depth. The only wrinkle is that the surface flux varies as the mixed layer cools. To get the temperature curve in Figure 9*a*, it was assumed that the far-field temperature for the boundary layer solution decreased at the same rate as the average temperature. This approach would tend to overestimate the cooling, because it ignores turbulent flux at the pycnocline which would both deepen and warm the mixing layer.

In the second case the mixing layer is allowed to deepen so as to keep the nondimensional PBL depth at 0.4. This adds an upward heat flux at the base of the layer, giving the average temperature equation the form

$$(d/dt)[h(\theta - \theta_0)] = -\langle w'\theta' \rangle|_0$$

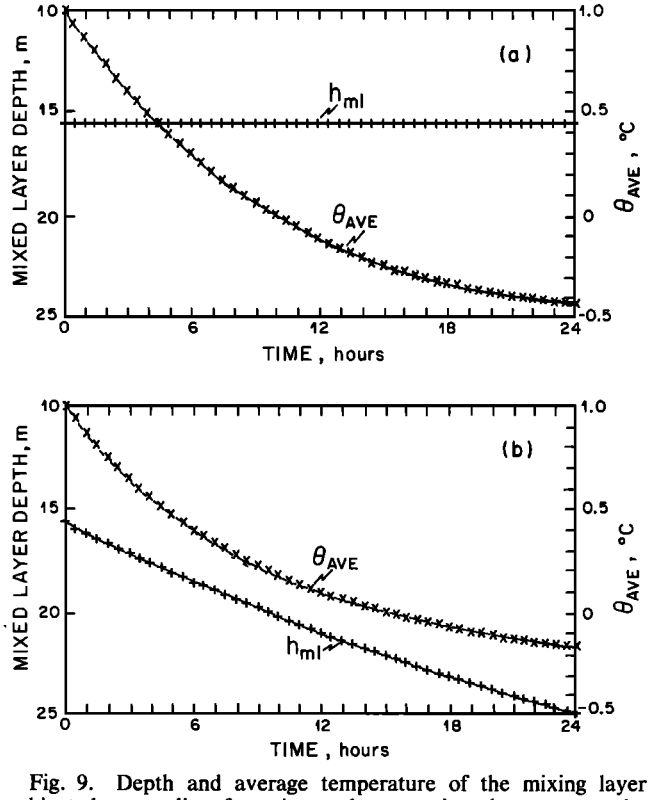

Fig. 9. Depth and average temperature of the mixing layer subjected to cooling from ice melt, assuming the ocean to be horizontally homogeneous. In Figure 9*a* the boundary layer depth is constant as determined by $\zeta_D = -0.4$ at the initial melting rate. In Figure 9*b* the boundary layer deepens to maintain $\zeta_D = -0.4$, entraining warmer water from below. Neither case is realistic because of mean current shear in the PBL.

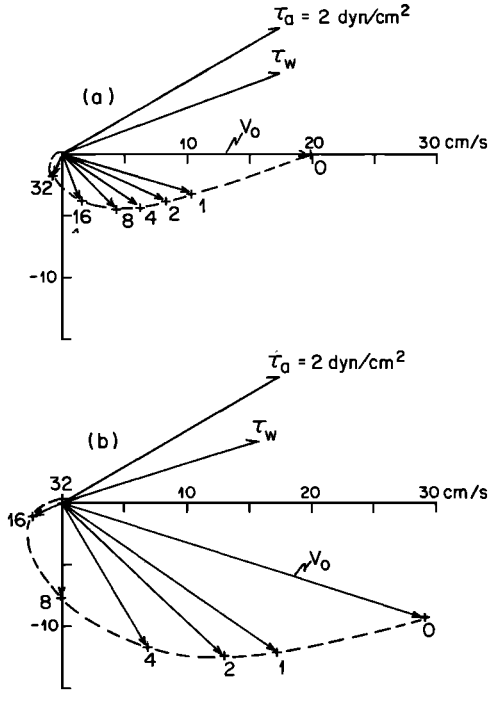

Fig. 10. Hodographs of ice drift and upper ocean currents for the same wind stress, with numbers indicating depth in meters. In Figure 10*a* there is no melting; in Figure 10*b* the ice drifts into water with $\Delta\theta = 1.5$ K. Note that as ice drifts across an abrupt front, cold water in the upper few meters is advected with it, enhancing the tendency for the leading edge to separate from the remaining pack.

where θ_0 is the initial temperature. The solution is shown in Figure 9*b*, where again the surface heat flux (melt rate) is calculated assuming the far-field temperature to decrease with the average. This approach neglects the stabilizing influence near the bottom of the mixed layer caused by the salinity decrease; thus it would probably overestimate the deepening and underestimate the cooling.

Before trying to extract too much information from this line of reasoning, however, it is well to consider another property of the boundary layer, namely, the mean shear. Figure 10 shows model hodographs (plan views) of the boundary layer velocity for the neutral case and for a rapid-melt regime, corresponding to the limits of Figure 8*a*. It is obvious that even if a sharp front did exist initially in the horizontal temperature field, it would be rapidly smeared in the vertical by PBL shear once the surface stress commenced. The ice following the leading edge would encounter cold water near the surface, despite the presence of warm water slightly deeper. The result would be to drive the zone of intense turbulent heat flux toward greater depths, presumably decreasing the tendency of the ice to 'grease' its own path by melting. It seems likely that advection of different water properties by turbulence-driven shear in the vicinity of the MIZ is often of equal or greater importance in determining the structure of the water column as the turbulent mixing itself.

4. SUMMARY

Sea ice that drifts in response to surface wind is embedded in a turbulent, rotating boundary layer. If ice begins to melt rapidly, the stabilizing influence of relatively fresh water at the top of the PBL will change both the heat flux and the momentum flux (drag). In this paper a theory for momentum flux in a planetary boundary layer stabilized by surface buoyancy has been extended to include turbulent flux of scalar contaminants in order to address a specific problem: what happens to sea ice when it is blown by wind into water at some known temperature above the melting point? Answering this question is a fundamental part of understanding how ice packs grow and decay.

The theory, which is a consistent extension of an approach that successfully describes many aspects of the stably stratified atmospheric boundary layer [*McPhee*, 1981], also appears to explain some important features of ice behavior in the marginal ice zone. It predicts rapid decay of ice in water only a degree or so above the melting point whenever there is much motion due to wind stress. It also provides a quantitatively realistic mechanism for divergence of the leading edge of an advancing ice pack that encounters warm water: a requirement of the formation of so-called 'ice edge bands.'

A notable departure of the new theory from extrapolations of laboratory heat flux studies is that the Stanton number falls rapidly with increasing $\Delta\theta$, so that, for example, ice moving at 30 cm s^{-1} in water with $\Delta\theta = 2$ K melts less than half again as fast (instead of twice as fast) as ice moving at the same speed with $\Delta\theta = 1$ K. A series of parameter studies made to identify which components of the model are critical in the MIZ context showed that probably the most important gap is knowledge of the turbulent Prandtl number ($1/\gamma_\theta$). If the primary interest is how far ice will drift (as opposed to how fast it will melt), then more knowledge of the effective surface roughness z_0 and its behavior in melting conditions is necessary. The relative impact of advection in the boundary layer vis-à-vis direct turbulent mixing is also an important part of understanding the thermal and haline properties of the upper ocean, as is knowledge of γ_s, the counterpart for salinity of γ_θ.

It is hoped that these points will be considered in designing field experiments. It may well turn out that the marginal ice zone serves as a very useful laboratory for studying properties of buoyancy effects in rotating boundary layers with application beyond understanding the drift and decay of sea ice.

NOTATION

$a = \beta\mu_*\eta_*$.
$b = (2k\xi n)^{-1/2}$
$b_1 = -1/\zeta_D$.
c_p specific heat of seawater.
f Coriolis parameter.
g acceleration of gravity.
h boundary layer thickness.
h_i ice thickness.
H nondimensional buoyancy flux.
$i = (-1)^{1/2}$.
k von Kármán's constant, equal to 0.4.
K_m eddy viscosity.
K_λ eddy diffusivity of contaminant.
K_* nondimensional eddy viscosity, equal to $fK_m/(u_*\eta_*)^2$.
l mixing length.
L Obukhov length, equal to $\rho_0 u_*^3/(gk\langle\rho' w'\rangle|_0)$.
L_i latent heat of fusion for sea ice.
Q_θ kinematic latent heat, equal to $\rho_i L_i/(\rho_0 c_p)$.
$Q_s = [S_w - (\rho_i/\rho_0)S_i]/1000$.

R_c critical flux Richardson number, equal to 0.2.
Re Reynolds number.
S_i salinity of ice.
S_w salinity of water.
$\hat{T}$ nondimensional stress (complex).
$\hat{U}$ water velocity (complex).
$\hat{U}_0$ surface (ice) velocity (complex).
$\hat{u}$ nondimensional ice velocity (complex).
$\hat{u}_0$ nondimensional surface velocity (complex).
$\hat{u}_*$ friction velocity (complex).
w vertical fluid velocity component.
z vertical coordinate.
z_0 surface roughness of ice underside.
$\alpha_s = \partial\rho/\partial s$.
α_θ coefficient of thermal expansion.
$\beta = (1 - \eta_*)(1/R_c + 1/\mu_*\xi_n)$.
γ_λ ratio of eddy diffusivity of λ to eddy viscosity.
$\hat{\delta}$ complex attenuation coefficient, equal to $(i/k\xi_N)^{1/2}$.
ζ nondimensional vertical coordinate.
ζ_D nondimensional planetary boundary layer length.
ζ_0 nondimensional surface roughness.
η_* stability parameter, equal to $(1 + \xi_N u_*/R_c fL)$.
Λ nondimensional scalar contaminant.
λ arbitrary scalar contaminant.
λ_* scale for λ.
Θ nondimensional temperature.
θ temperature.
$\mu_* = u_*/fL$.
ξ_N dimensionless planetary boundary layer constant, equal to 0.052.
ρ density.
$\hat{\tau}$ stress (complex).

Acknowledgment. This work was supported by the Office of Naval Research, grant N-00014079-C0004 to the Polar Science Center, University of Washington.

REFERENCES

Ashton, G. D., Turbulent heat transfer to wavy boundaries, in *Heat Transfer and Fluid Mechanics Institute Proceedings*, pp. 200–213, Stanford University Press, Stanford, Calif., 1972.

Griffin, O. M., Heat, mass and momentum transfer effects on the ablation of icebergs in seawater, in *Iceberg Utilization*, edited by A. A. Husseiny, pp. 229–244, Pergamon, New York, 1978.

Hinze, J., *Turbulence*, 2nd ed., 790 pp., McGraw-Hill, New York, 1975.

Martin, S., P. Kauffman, and C. Parkinson, The movement and decay of ice edge bands in the winter Bering Sea (abstract), *Eos Trans. AGU, 62*, 895, 1981.

McPhee, M. G., The effect of the oceanic boundary layer on the mean drift of pack ice: Application of a simple model, *J. Phys. Oceanogr., 9*, 388–400, 1979.

McPhee, M. G., An analytic similarity theory for the planetary boundary layer stabilized by surface buoyancy, *Boundary Layer Meteorol., 21*, 325–339, 1981.

McPhee, M. G., The upper ocean, in *Air-Sea-Ice Interaction*, edited by N. Untersteiner, NATO Advanced Study Institute, Maratea, Italy, in press, 1982.

McPhee, M. G., and J. D. Smith, Measurements of the turbulent boundary layer under pack ice, *J. Phys. Oceanogr., 6*, 696–771, 1976.

Neumann, G., and W. J. Pierson, Jr., *Principles of Physical Oceanography*, 545 pp., Prentice-Hall, Englewood Cliffs, N. J., 1966.

Paquette, R. G., and R. H. Bourke, Temperature fine structure near the sea-ice margin of the Chukchi Sea, *J. Geophys. Res., 84*, 1155–1164, 1979.

Pease, C., Eastern Bering Sea processes, *Mon. Weather Rev., 108*, 2016–2023, 1980.

Schwerdtfeger, P., The effect of finite heat content and thermal diffusion on the growth of a sea-ice cover, *J. Glaciol., 5*, 315–324, 1964.

Turner, J. S., *Buoyancy Effects in Fluids*, 367 pp., Cambridge University Press, New York, 1973.

Zilitinkevich, S. S., Resistance laws and prediction equations for the depth of the planetary boundary layer, *J. Atmos. Sci., 32*, 741–752, 1975.

(Received May 17, 1982;
revised July 19, 1982;
accepted August 23, 1982.)